Nanoscale

COMMUNICATION

View Article Online
View Journal | View Issue

Cite this: *Nanoscale*, 2015, **7**, 20369

Received 6th September 2015,
Accepted 9th November 2015

DOI: 10.1039/c5nr06095h

www.rsc.org/nanoscale

Inclusion of Cu nano-cluster 1D arrays inside a C_3-symmetric artificial oligopeptide *via* co-assembly†

Ruiying Gong, Fei Li, Chunpeng Yang and Xiaobo Wan*

A peptide sequence N_3-GVGV-OMe (G: glycine; V: valine) was attached to a benzene 1,3,5-tricarboxamide (BTA) derivative *via* "click chemistry" to afford a C_3-symmetric artificial oligopeptide. The key feature of this oligopeptide is that the binding sites (triazole groups formed by click reaction) are located at the center, while the three oligopeptide arms with a strong tendency to assemble are located around it, which provides inner space to accommodate nanoparticles *via* self-assembly. The inclusion of Cu nanoclusters and the formation of one-dimensional (1D) arrays inside the nanofibers of the C_3-symmetric artificial oligopeptide assembly were observed, which is quite different from the commonly observed nanoparticle growth on the surface of the pre-assembled oligopeptide nanofibers *via* the coordination sites located outside. Our finding provides an instructive concept for the design of other stable organic–inorganic hybrid 1D arrays with the inorganic nanoparticles inside.

The synthesis and assembly of one-dimensional (1D) metallic nanoparticles assisted by bio-organic molecules are interesting topics in nano science. In particular, protein or peptide directed metallic nanoparticle assembly has attracted much attention in the past few decades due to the versatility of the peptide pool, the mild preparation conditions, the controllable sizes and shapes of the resultant nano-structures, and the specific functions resulting from the hybridization of metallic and organic functionalities, which were summarized in recent reviews.[1–5] In many cases, the metallic nanoparticles are immobilized on the surface of the assembled peptide nanofibers, *via* specific interactions such as ligand–metal complexation and electrostatic attraction. For instance, Matsui and co-workers reported Cu nano-crystal growth on a bolaamphiphile peptide nanotube, the surface of which is pre-modified with a sequenced histidine-rich peptide.[6] The interaction between the histidine moiety and Cu provided the driving force for the assembly. Pochan *et al.* reported 1D assembly of negatively charged Au nanoparticles onto the surface of 17H6 nanofibrils by neutralizing the positively-charged histidine moiety on the peptide.[7] This concept was widely used in the preparation of other 1D metallic or inorganic nanoparticle assemblies.[8–18] On the other hand, the inclusion of metallic nanoparticles inside proteins or peptides to form the 1D structure was realized mainly through the capillary effects but was scarcely reported. Reches and Gazit reported the *in situ* reduction of Ag^+ ions filled inside diphenylalanine (Di-Phe) nanotubes to form Ag nanowires.[19] The incorporation of Fe_3O_4 nanoparticles inside a bolaamphiphile peptide at low concentration has also been reported.[9] Due to the non-specific nature of the capillary effects, the nanowire/nanoparticle growth inside the tube may coexist with the nanoparticle growth on the surface in the presence of other interactions.[20–22] The reports on inclusion of metal nanoparticles through specific interactions inside the peptides are rare. One recent example is to use electrostatic attraction to immobilize $AuCl_4^-$ inside a peptide, which was further reduced *in situ* to give Au nanoparticles inside to form nanoribbons.[23] Here we wish to report the simultaneous inclusion of Cu nano-clusters inside a C_3-symmetric artificial oligopeptide assembly through ligand–metal complexation to form 1D arrays. The key feature of these oligopeptides is that the binding sites are located at the center, while the three oligopeptide arms with a strong tendency to assemble are located around it, which provides space to accommodate nanoparticles *via* self-assembly. This concept might be instructive for the design of other stable novel 1D nanoparticle arrays.

The C_3-symmetric artificial oligopeptide was constructed from two components by click chemistry: one is an oligopeptide with a terminal azide group which has a strong tendency to form a β-sheet, namely N_3-GVGV-OMe,[24] and the other one is a benzene 1,3,5-tricarboxamide (BTA) derivative with a terminal alkynyl group. BTA is a versatile building block for self assembly[25] and was used to form chiral nano-assemblies for asymmetric catalysis recently.[26] The growth of Au nano-

CAS Key Laboratory of Bio-based Materials, Qingdao Institute of Bioenergy and Bioprocess Technology, Chinese Academy of Sciences, 189 Songling Road, Qingdao, Shandong Province 266101, P. R. China. E-mail: wanxb@qibebt.ac.cn

†Electronic supplementary information (ESI) available: Detailed synthesis, gel preparation, general methods for characterization, and the characterisation of BTA-C_3-GVGVOMe assembly including or not including Cu nano-cluster arrays. See DOI: 10.1039/c5nr06095h

particles on the surface of such assemblies was also reported.[27] The BTA–oligopeptide conjugate was first reported by Matsuura *et al*. and the formation of nanofibers consisting of β-sheets was observed.[28] The click reaction between N_3-GVGV-OMe **1** and *N*,*N*′,*N*″-tris-propargyl benzene-1,3,5-tricarboxamide **2** proceeded smoothly to give the C_3-symmetric artificial oligopeptide **3** (BTA-C_3-GVGVOMe) in excellent yield and also installed three triazole groups between the BTA core and the oligopeptide arms, as shown in Scheme 1. Details of the synthesis and characterization are reported in the ESI.† The analytical and spectroscopic data for oligopeptide **3** are fully consistent with its molecular structure.

BTA-C_3-GVGVOMe showed good solubility in hot DMF/MeOH, and gradually formed an organogel during storage. The assembly of purified BTA-C_3-GVGVOMe is conducted through a colloidal self-assembly method. In a typical experiment, oligopeptide **3** (0.01 g, 0.006 mmol) was dissolved in DMF/MeOH (120 μL, 5 : 1 volume ratio) at 65 °C and then incubated at 36 °C for about 30 days to form a stable gel. Scanning electron microscopy (SEM) images show that the purified artificial peptide assembles into nanofibers up to several micrometers long with widths ranging from 20 to 100 nm under low scanning voltage (3 kV) (Fig. S1†). The transmission electron microscopy (TEM) images of the purified artificial peptide **3** (Fig. 1a and S2†) also confirmed the formation of these nanofibers.

Surprisingly, if BTA-C_3-GVGVOMe was not thoroughly purified (there were some residual catalysts ($CuSO_4{\cdot}5H_2O$) and ascorbic acid), the formation of aligned nanoparticles along the axis of the nanofibers (Fig. 1b) was observed under the same preparation conditions. Furthermore, different from many previous reports, these nanoparticles seem to be located inside the nanofibers, since the edge of the nanofibers is smooth and no growth of the nano-particles on the edge was observed (as indicated by the arrows in Fig. 1c). The difference

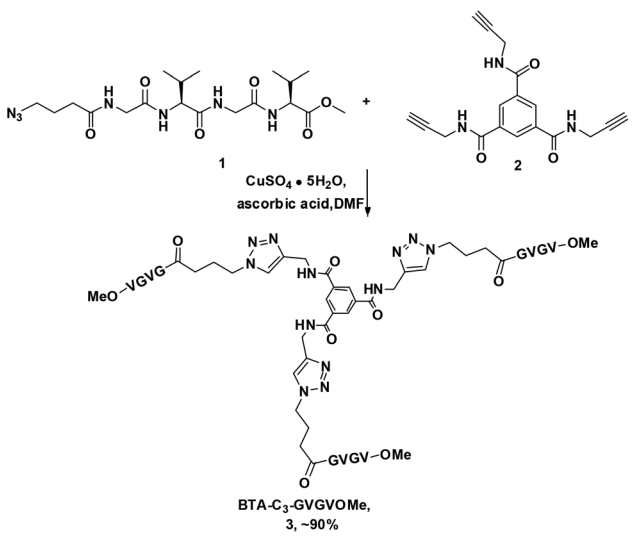

Scheme 1 Synthesis route of BTA-C_3-GVGVOMe **3**.

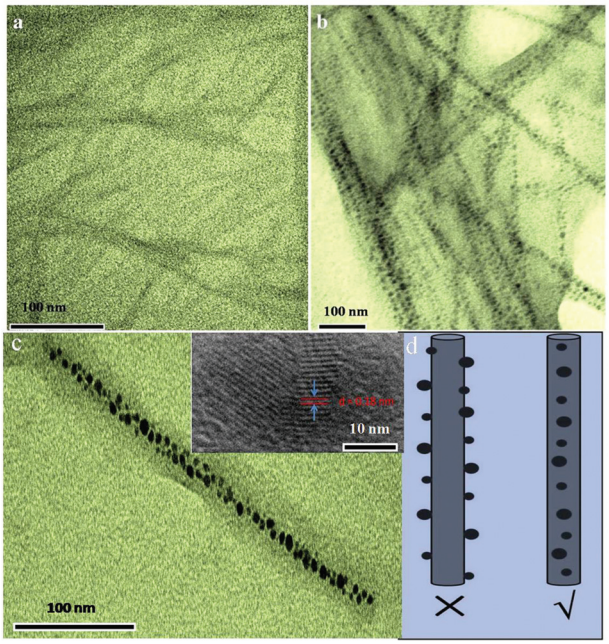

Fig. 1 TEM images of the assembly morphology of gel@BTA-C_3-GVGVOMe (a) and gel@BTA-C_3-GVGVOMe & Cu (b). (c) Enlarged TEM image of one-dimensional Cu nanocluster array. (d) Schematic diagram of Cu nanoclusters aligned along the nanostructured gel fibers.

between the two types of alignments is the schematic denoted in Fig. 1d. The size of the nanoparticles ranges from 5 to 10 nm. We reasoned that the nanoparticles should be Cu(0) clusters, since Cu(II) could be reduced to Cu(0) in the presence of ascorbic acid. Indeed, ascorbic acid is a mild reducing reagent in the preparation of many metallic nano-materials including Cu(0).[29] High-resolution TEM image (the insert in Fig. 1c, full image in Fig. S3†) clearly shows that the nanoparticles inside the artificial oligopeptide are crystalline, with a *d* space around 0.18 nm, which corresponds to the (200) plane of Cu(0). X-ray photoelectron spectroscopy (XPS) of the xerogel showed two peaks at 954.7 eV and 932.6 eV, which also correspond to Cu2p1/2 and Cu2p3/2 of Cu(0), respectively (Fig. S4†).

The role of ascorbic acid in the formation of Cu(0) 1D arrays inside the C_3-symmetric oligopeptide **3** was confirmed in a control experiment. If the purified oligopeptide **3** was incubated just with $CuSO_4{\cdot}5H_2O$ under the same conditions for gel formation, no Cu(0) nanoparticle formation was observed. This is understandable since the oligopeptide itself does not have the reductive center to reduce Cu(II). On the other hand, when the purified oligopeptide **3** was incubated with $CuSO_4{\cdot}5H_2O$ and ascorbic acid, the formation of the Cu(0) 1D arrays inside the nanofibers was re-observed. Furthermore, the amount of Cu(0) incorporated into the oligopeptide nanofibers could be modulated by changing the molar feeding ratio of Cu(II) toward the oligopeptide. Three feeding ratios (0.6 : 1; 1.2 : 1; 2.4 : 1) were set and the TEM images of the obtained Cu(0)–oligopeptide nanofibers are listed in Fig. 2.

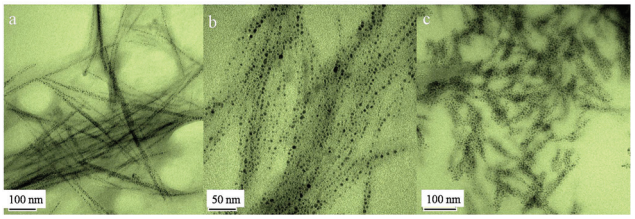

Fig. 2 TEM images of the assembly morphology of gel@BTA-C_3-GVGVOMe & Cu at different Cu : oligopeptide molar ratios. (a) 0.6 : 1; (b) 1.2 : 1, (c) 2.4 : 1. In each case, the molar content of the ascorbic acid is twice as much as that of $CuSO_4 \cdot 5H_2O$.

When 0.6 equiv. of Cu(II) was incubated with oligopeptide in the presence of ascorbic acid (Fig. 2a), the nanofibers with Cu(0) nanoparticles inside are very similar to that obtained from not well-purified oligopeptides. When the molar ratio of Cu(II) was increased to 1.2 equiv. or higher, these nanofibers tended to aggregate into larger but shorter bundles.

The formation of Cu nanoparticle arrays inside the oligopeptide fiber was further confirmed by SEM at elevated voltage. In the low-voltage (3 kV) SEM technique, electrons interact with the surface of the specimen, and the corresponding images are more sensitive to the chemical and topographic form of the surface. In the conventional voltage region (10 to 30 kV), the SEM images reflect more about the structure of the bulk.[30] Furthermore, due to the heavy-atom effects, Cu should have a stronger signal in SEM than the peptides. The comparison of the SEM images of organogel obtained from BTA-C_3-GVGVOMe and BTA-C_3-GVGVOMe &Cu (obtained at 2.4 equiv. Cu(II) feeding ratio) at different scanning voltages is shown in Fig. 3. At 3 kV scanning voltage, both gels showed similar SEM images (nanofibers with similar brightness, Fig. 3a and c), indicating that the surfaces of both nanofibers might be composed of similar elements. At 20 kV scanning voltage, the image of the nanofiber of BTA-C_3-GVGVOMe (Fig. 3b) did not show much difference from that obtained at 3 kV voltage, inferring that the elements (C, N, O atoms from the oligopeptides) in the bulk showed little difference from those on the surfaces of the nanofibers. On the other hand, the images of BTA-C_3-GVGVOMe &Cu nanofibers obtained at 20 kV exhibit many dazzling nanofibers with enhanced brightness (Fig. 3d and S5a–d†), which are assigned to the Cu(0) arrays inside the oligopeptide nanofibers. Two enlarged images of the dazzling nanofibers are shown in the inset of Fig. 3d and S5d,† and the smooth edge of these nanofibers further implied that no Cu nanoparticles were immobilized on the surface.

The inclusion of Cu(0) nanoparticles inside the three-armed peptides makes those nanoparticles stable for long-term storage. Fig. S6† showed the image of the assembled nano-fibers which have been stored on the shelf for 2 years. No aggregation of these nanoparticles was observed.

Based on these results, the mechanism of self-assembly of Cu(0)–oligopeptide nanofibers was proposed, and is shown in

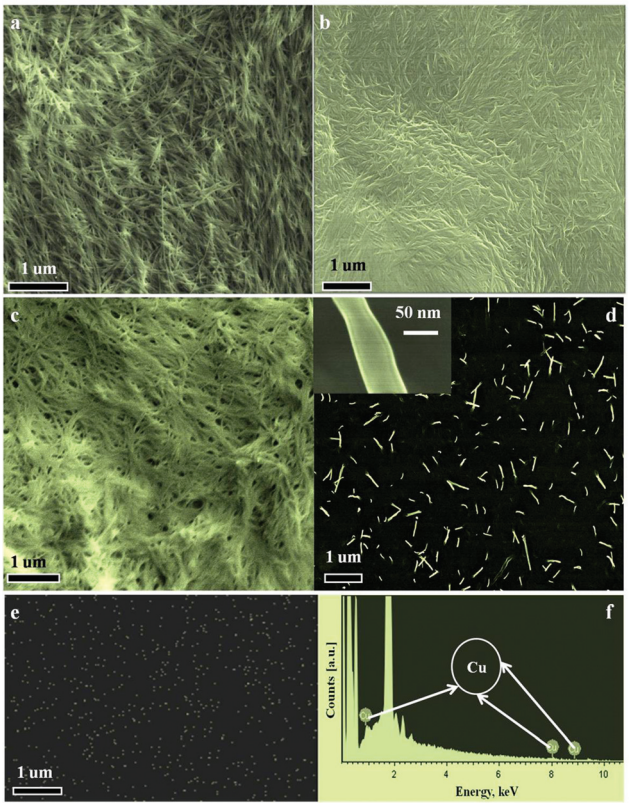

Fig. 3 SEM images of the assembly morphology of gel@BTA-C_3-GVGVOMe (a: at 3 kV scanning voltage) and (b: at 20 kV scanning voltage). (c) and (d) are the SEM images of the assembly morphology of gel@BTA-C_3-GVGVOMe & Cu obtained at 2.4 equiv. of Cu(II) at 3 kV scanning voltage and at 20 kV scanning voltage, respectively. (e) The elemental map for Cu in the image (d). (f) The energy dispersive spectrometer (EDS) of Cu in the image (d).

Fig. 4. As stated earlier, the most important feature of BTA-C_3-GVGVOMe is that the triazole groups located inside act as the coordination center and the oligopeptide with a strong tendency for self-assembly at the periphery acts as the assembly center. The complexation of the triazole group with Cu(II) has been well documented,[31] and therefore it is reasonable to postulate that the Cu(0) nanoparticles were formed either through the formation of the Cu(II)-triazole complex during the incubation period followed by the reduction by ascorbic acid, or the reduction first then followed by coordination, or these two processes occurring simultaneously. To prove this, a control experiment was carried out to co-assemble the pre-synthesized Cu nanocluster with the purified oligopeptide. Cu nanocluster was prepared by mixing ascorbic acid and $CuSO_4 \cdot 5H_2O$ in a solution of DMF/MeOH. A series of TEM images (Fig. S8a–f†) showed these Cu nanoclusters exist either in individual form or in aggregated form. We identified that the Cu nanoclusters were composed of Cu(0) *via* high-resolution TEM (Fig. S9†). A stable gel was prepared after the addition of the purified BTA-C_3-GVGVOMe into the pre-synthesized Cu clusters followed by incubation in a solution of DMF/MeOH. The formation of an ordered Cu nanoparticle array inside the oligo-

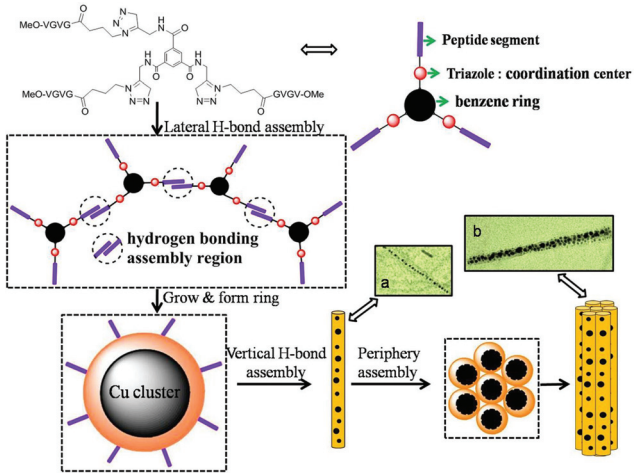

Fig. 4 Plausible stacking model for one-dimensional Cu nanocluster arrays directed by the assembly from BTA-C_3-GVGVOMe.

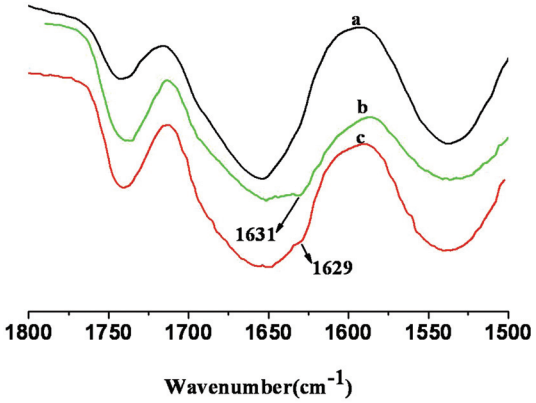

Fig. 5 The amide I region of the FTIR spectra: (a) the powder of BTA-C_3-GVGVOMe & Cu, (b) xerogel of BTA-C_3-GVGVOMe, (c) xerogel of BTA-C_3-GVGVOMe & Cu.

peptide fiber was observed in TEM images (Fig. S10a and b†). This observation confirmed that the ordered Cu(0) nanoparticle arrays could be formed in advance before it was organized into 1-D arrays in the presence of the peptides.

According to the plausible stacking model in Fig. 4, we speculated that the oligopeptide could firstly be assembled by lateral H-bonds and grow to form rings, at the same time Cu clusters are formed during the formation of these rings due to the complexation of triazole groups. Here, we elaborately studied the evolution of Cu(0) 1D arrays inside the C_3-symmetric oligopeptide **3** with the gelation time (the time taken by the oligopeptide assembled by H-bonds to form a stable gel) by controlling the gelation temperature (see Fig. S7†). The experimental results disclosed that there is a strong dependence of Cu(0) 1D arrays inside the C_3-symmetric oligopeptide **3** on the gelation time. When the gelation time is very fast (2 days, Fig. S7a†), no Cu(0) 1D arrays could be found. With the increase of the gelation time, more and more Cu(0) 1D arrays could be seen (Fig. S7b–d†). This means that the formation of Cu clusters must be in step with the formation of these rings, or it is very difficult for the Cu clusters to move into the inside cavity once the oligopeptides has assembled. Furthermore, the oligopeptide could form long fibers by vertical H-bond assembly and form a Cu cluster string (Fig. 4a). Finally the single fibers bunch together to form larger bundles (Fig. 4b).

BTA-C_3-GVGVOMe might assemble into rings *via* β-sheet formation which provides the cavity to accommodate Cu(0) nanoparticles. Fourier transform infrared spectroscopy (shown in Fig. 5) gives some evidence for the formation of the β-sheet. In contrast to the FTIR spectrum of BTA-C_3-GVGVOMe & Cu powder (Fig. 5a), the FTIR spectrum of the xerogel of pure BTA-C_3-GVGVOMe (Fig. 5b) showed an obvious peak at 1631 cm^{-1}, which is evidence of β-sheet formation. This indicates that the incubation of the artificial oligopeptide is necessary to promote the formation of β-sheets. Although not obvious, the FTIR spectrum of the xerogel of BTA-C_3-GVGVOMe & Cu (Fig. 5c) also showed a shoulder peak at 1629 cm^{-1}, which confirmed the formation of β-sheets in this organic–inorganic hybrid. The difference of the intensity of this characteristic peak might be due to the interference of the nanoparticles in the β-sheet formation which changed the ratio between β-sheets and other types of secondary structures of the oligopeptide. Furthermore, the oligopeptide sidechain stretching out from such rings might form H-bonding with other hexagonal or octagonal rings to form more complex nanostructures, and the stacking of such ring systems results in the formation of nanofibers with Cu(0) nanoparticles inside. The nanofibers further aggregate by forming H-bonding with each other through the oligopeptide arms stretching out from these nanofibers to pack into nanofiber bundles, so the 1D Cu nanoparticle arrays also packed into the bundles. Moreover, with the increase of Cu(0) content, the nanoparticles may also interact with triazole groups stretching out from the rings to form even larger bundles, which accounts for the topology evolution of these nanofibers when the amount of Cu(II) was increased.

In summary, we found that by introducing coordination sites at the center of a C_3-symmetric artificial oligopeptide, Cu(0) nanoparticle 1D arrays formed inside the nanofibers composed of such oligopeptides. Different from other peptide templates with the coordination center outside which allows the growth of inorganic nanoparticles outside the nano-assembly, this result provides a novel concept to fabricate 1D biomaterials with inorganic elements incorporated inside, which might have potential applications such as surface-insulated conducting nanowires. We believe that by tuning the structure of the coordination center and the structure of the self-assembly periphery, the incorporation of other metals and inorganic nanoparticles into such biomaterials could be realized. Although this assembly process occurs in the organic solvent system, the extension to a more environment-friendly aqueous system is also possible by structural modification. Such work is currently underway in our laboratory.

Acknowledgements

The authors thank the "100 Talents Program" from the Chinese Academy of Sciences, the National Natural Science Foundation of China (51403228) for financial support.

Notes and references

1 N. Ma, E. H. Sargent and S. O. Kelley, *J. Mater. Chem.*, 2008, **18**, 954–964.
2 E. Gazit, *FEBS J.*, 2007, **274**, 317–322.
3 M. B. Dickerson, K. H. Sandhage and R. R. Naik, *Chem. Rev.*, 2008, **108**, 4935–4978.
4 C.-L. Chen and N. L. Rosi, *Angew. Chem., Int. Ed.*, 2010, **49**, 1924–1942.
5 R. de la Rica and H. Matsui, *Chem. Soc. Rev.*, 2010, **39**, 3499–3509.
6 I. A. Banerjee, L. T. Yu and H. Matsui, *Proc. Natl. Acad. Sci. U. S. A.*, 2003, **100**, 14678–14682.
7 N. Sharma, A. Top, K. L. Kiick and D. J. Pochan, *Angew. Chem., Int. Ed.*, 2009, **48**, 7078–7082.
8 R. Djalali, Y.-F. Chen and H. Matsui, *J. Am. Chem. Soc.*, 2003, **125**, 5873–5879.
9 I. A. Banerjee, L. Yu, M. Shima, T. Yoshino, H. Takeyama, T. Matsunaga and H. Matsui, *Adv. Mater.*, 2005, **17**, 1128–1131.
10 A. Banerjee Ipsita, L. Yu and H. Matsui, *J. Am. Chem. Soc.*, 2005, **127**, 16002–16003.
11 N. Nuraje, K. Su, A. Haboosheh, J. Samson, E. P. Manning, N. L. Yang and H. Matsui, *Adv. Mater.*, 2006, **18**, 807–811.
12 M. T. Kumara, B. C. Tripp and S. Muralidharan, *Chem. Mater.*, 2007, **19**, 2056–2064.
13 H. Bai, K. Xu, Y. Xu and H. Matsui, *Angew. Chem., Int. Ed.*, 2007, **46**, 3319–3322.
14 C.-L. Chen, P. Zhang and N. L. Rosi, *J. Am. Chem. Soc.*, 2008, **130**, 13555–13557.
15 A. Rehman, Z. A. Raza, R. Saifur, Z. M. Khalid, C. Subramani, V. M. Rotello and I. Hussain, *J. Colloid Interface Sci.*, 2010, **347**, 332–335.
16 M. Shi, W. Su and H. Matsui, *Nanoscale*, 2010, **2**, 2373–2376.
17 H. Xu, Y. Wang, X. Ge, S. Han, S. Wang, P. Zhou, H. Shan, X. Zhao and J. R. Lu, *Chem. Mater.*, 2010, **22**, 5165–5173.
18 C. Zhang, C. Song, H. C. Fry and N. L. Rosi, *Chem. – Eur. J.*, 2014, **20**, 941–945.
19 M. Reches and E. Gazit, *Science*, 2003, **300**, 625–627.
20 O. Carny, D. E. Shalev and E. Gazit, *Nano Lett.*, 2006, **6**, 1594–1597.
21 P. Ramasamy, S. Guha, E. S. Shibu, T. S. Sreeprasad, S. Bag, A. Banerjee and T. Pradeep, *J. Mater. Chem.*, 2009, **19**, 8456–8462.
22 P. Koley and A. Pramanik, *Adv. Funct. Mater.*, 2011, **21**, 4126–4136.
23 K.-Y. Tomizaki, S. Wakizaka, Y. Yamaguchi, A. Kobayashi and T. Imai, *Langmuir*, 2014, **30**, 846–856.
24 R. Y. Gong, Y. B. Song, Z. X. Guo, M. Li, Y. Jiang and X. Wan, *Supramol. Chem.*, 2013, **25**, 269–275.
25 S. Cantekin, T. F. A. de Greef and A. R. A. Palmans, *Chem. Soc. Rev.*, 2012, **41**, 6125–6137.
26 M. Raynal, F. Portier, P. W. N. M. van Leeuwen and L. Bouteiller, *J. Am. Chem. Soc.*, 2013, **135**, 17687–17690.
27 S. H. Jung, J. Jeon, H. Kim, J. Jaworski and J. H. Jung, *J. Am. Chem. Soc.*, 2014, **136**, 6446–6452.
28 K. Matsuura, K. Murasato and N. Kimizuka, *J. Am. Chem. Soc.*, 2005, **127**, 10148–10149.
29 H. Yang, S. W. Finefrock, J. D. Albarracin Caballero and Y. Wu, *J. Am. Chem. Soc.*, 2014, **136**, 10242–10245.
30 D. C. Joy and C. S. Joy, *Micron*, 1996, **27**, 247–263.
31 P. M. Guha, H. Phan, J. S. Kinyon, W. S. Brotherton, K. Sreenath, J. T. Simmons, Z. Wang, R. J. Clark, N. S. Dalal, M. Shatruk and L. Zhu, *Inorg. Chem.*, 2012, **51**, 3465–3477.